

An unidentified TeV source in the vicinity of Cygnus OB2

F. Aharonian¹, A. Akhperjanian⁷, M. Beilicke⁴, K. Bernlöhr¹, H. Börst⁵, H. Bojahr⁶, O. Bolz¹, T. Coarasa², J. Contreras³, J. Cortina², S. Denninghoff², V. Fonseca³, M. Girma¹, N. Götting⁴, G. Heinzlmann⁴, G. Hermann¹, A. Heusler¹, W. Hofmann¹, D. Horns¹, I. Jung¹, R. Kankanyan¹, M. Kestel², J. Kettler¹, A. Kohnle¹, A. Konopelko¹, H. Kornmeyer², D. Kranich², H. Krawczynski⁹, H. Lampeitl⁴, M. Lopez³, E. Lorenz², F. Lucarelli³, N. Magnussen¹⁰, O. Mang⁵, H. Meyer⁶, M. Milite⁴, R. Mirzoyan², A. Moralejo³, E. Ona³, M. Panter¹, A. Plyasheshnikov^{1,8}, J. Prahl⁴, G. Pühlhofer¹, G. Rauterberg⁵, R. Reyes², W. Rhode⁶, J. Ripken⁴, A. Röhring⁴, G. P. Rowell¹, V. Sahakian⁷, M. Samorski⁵, M. Schilling⁵, F. Schröder⁶, M. Siems⁵, D. Sobzynska², W. Stamm⁵, M. Tluczykont⁴, H.J. Völk¹, C. A. Wiedner¹, W. Wittek² (HEGRA Collaboration), Y. Uchiyama¹¹, T. Takahashi¹¹

¹ Max-Planck-Institut für Kernphysik, Postfach 103980, D-69029 Heidelberg, Germany

² Max-Planck-Institut für Physik, Föhringer Ring 6, D-80805 München, Germany

³ Universidad Complutense, Facultad de Ciencias Físicas, Ciudad Universitaria, E-28040 Madrid, Spain

⁴ Universität Hamburg, Institut für Experimentalphysik, Luruper Chaussee 149, D-22761 Hamburg, Germany

⁵ Universität Kiel, Institut für Experimentelle und Angewandte Physik, Leibnizstraße 15-19, D-24118 Kiel, Germany

⁶ Universität Wuppertal, Fachbereich Physik, Gaußstr.20, D-42097 Wuppertal, Germany

⁷ Yerevan Physics Institute, Alikhanian Br. 2, 375036 Yerevan, Armenia

⁸ On leave from Altai State University, Dimitrov Street 66, 656099 Barnaul, Russia

⁹ Now at Washington University, St. Louis MO 63130, USA

¹⁰ Now at IFAE, Universitat Autònoma de Barcelona, Spain

¹¹ Institute of Space and Astronautical Science, 3-1-1 Yoshinodai, Sagamihara, Kanagawa 229-8510, Japan

Received / Accepted

Abstract. Deep observation (~ 113 hrs) of the Cygnus region at TeV energies using the HEGRA stereoscopic system of air Čerenkov telescopes has serendipitously revealed a signal positionally inside the core of the OB association Cygnus OB2, at the edge of the 95% error circle of the EGRET source 3EG J2033+4118, and $\sim 0.5^\circ$ north of Cyg X-3. The centre of gravity of the source is RA α_{J2000} : $20^{\text{hr}} 32^{\text{m}} 07^{\text{s}} \pm 9.2'_{\text{stat}} \pm 2.2'_{\text{sys}}$, Dec δ_{J2000} : $+41^\circ 30' 30'' \pm 2.0'_{\text{stat}} \pm 0.4'_{\text{sys}}$. The source is steady, has a post-trial significance of $+4.6\sigma$, indication for extension with radius $5.6'$ at the $\sim 3\sigma$ level, and has a differential power-law flux with hard photon index of $-1.9 \pm 0.3_{\text{stat}} \pm 0.3_{\text{sys}}$. The integral flux above 1 TeV amounts $\sim 3\%$ that of the Crab. No counterpart for the TeV source at other wavelengths is presently identified, and its extension would disfavour an exclusive pulsar or AGN origin. If associated with Cygnus OB2, this dense concentration of young, massive stars provides an environment conducive to multi-TeV particle acceleration and likely subsequent interaction with a nearby gas cloud. Alternatively, one could envisage γ -ray production via a jet-driven termination shock.

Key words. Gamma rays: observations - Stars: early-type - Galaxy: open clusters and associations: individual: Cygnus OB2

1. Introduction

The current generation of ground-based imaging atmospheric Čerenkov telescopes offer coverage of the multi GeV to TeV γ -ray sky at centi-Crab sensitivity and arc-minute resolution. In particular, stereoscopy employed by the HEGRA CT-System at La Palma (Daum et al. 1997) offers highly accurate reconstruction of event directions at

angles up to $\sim 3^\circ$ off-axis. Results here are taken from data originally devoted to Cyg X-3, and the EGRET source GeV J2035+4214 (Lamb & Macomb 1997). The separation between these objects ($\sim 1.5^\circ$) permits a combined analysis given the overlap in their CT-System fields of view (FOV). In this letter we present analysis details and observational properties of a serendipitously discovered TeV source in these data with some emphasis given to comparing two different background models. Brief discus-

Send offprint requests to: G.P. Rowell, D. Horns

e-mail: Gavin.Rowell@mpi-hd.mpg.de, Dieter.Horns@mpi-hd.mpg.de

sion concerning astrophysical origins and location of this new source is also presented.

2. Data Analysis and Results

The HEGRA system of imaging atmospheric Čerenkov telescopes (IACT-System), consists of 5 identical telescopes operating in coincidence for the stereoscopic detection of air showers induced by primary γ -rays in the atmosphere. In data dedicated to Cyg X-3, alternate ~ 20 minute runs targeting the Cyg X-3 position $\pm 0.5^\circ$ in declination were taken during moonless nights of Aug-Sept 1999, Sept-Oct 2000 and Jun-Oct 2001. Likewise in data dedicated to GeV J2035+4124, ~ 20 minute runs were obtained tracking directly the GeV source during Jul-Aug 2001. In total, three tracking positions are present in combined data. For data quality, runs and certain events were rejected according to well-defined criteria, the most critical being a background event rate < 10 Hz for zenith angles $< 45^\circ$ (10 Hz is $> 70\%$ of the typical maximum rate), leaving a total of 112.9 hours data for analysis. Preferential selection of γ -ray-like events (against the cosmic-ray background) is achieved by using the difference between the reconstructed and assumed event direction, θ , and the mean-scaled-width parameter, \bar{w} (Konopelko 1995). In searching for weak point-like and marginally extended sources, so-called tight cuts are considered optimal given the angular resolution of the CT-System ($< 0.1^\circ$): $\theta < 0.12^\circ$ and $\bar{w} < 1.1$, where we use algorithm '3' as described by Hofmann et al. (1999) for the event direction reconstruction. The number of images per event, n_{tel} , used for calculating θ and \bar{w} was also *a priori* chosen at $n_{\text{tel}} \geq 3$. Monte Carlo simulations (Konopelko et al. 1999) and tests on real sources have shown that $n_{\text{tel}} = 2$ events contribute little to the overall sensitivity.

2.1. Source Search and Background Estimates

In searching for new TeV sources, *skymaps* of event direction excesses over the RA & Dec plane are generated after having estimated the background over the FOV. A new empirically-based *template* background model has been developed with the goal of simple generation of skymaps and source identification. It is based on the estimation of a background template comprising events normally rejected according to the \bar{w} criterion. Based on tight \bar{w} cuts, we define the number of events in the γ -ray regime s from $\bar{w} < 1.1$, and for the template background b from $1.3 < \bar{w} < 1.5$. A necessary correction applied to the template background, accounts for differences in the radial profile between the two \bar{w} regimes. A normalisation α , to derive excess events $s - \alpha b$ at position in the FOV, accounts for differences in the total number of events in the two \bar{w} regimes. A systematic error in the excess ($s - \alpha b$) of $\sim 0.05\alpha b$ is estimated from differences in large-scale ($\sim 1^\circ \times 1^\circ$) 'hot' and 'cold' regions in the FOV. The template model permits an estimate of the background over the entire FOV without requiring separate observations of

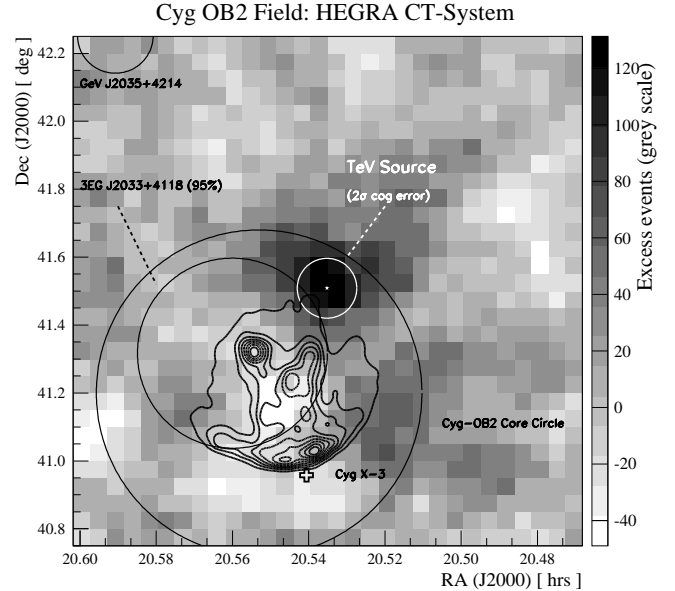


Fig. 1. Skymap ($1.5^\circ \times 1.5^\circ$ view at $0.05^\circ \times 0.05^\circ$ binning) of excess events $s - \alpha b$, using the template background model. At each bin, the excess is estimated from events within a radius $\theta = 0.12^\circ$. Included are 95% error circles of various EGRET sources, the core of Cygnus OB2 defined by Knödlseider (2000), the TeV COG (star) and its 2σ error circle, and the location of Cyg X-3. ASCA GIS contours (2-10 keV) are overlaid.

off-source positions. It has been tested on a variety of CT-System data containing strong, weak and no γ -ray signals, and found consistent with more conventional background models discussed below (see Rowell 2002 for a full description). Fig. 1 presents the resulting skymap where at each bin the excess is calculated from events summed within a circle of radius $\theta = 0.12^\circ$, for each \bar{w} regime. The template model was used in discovering the TeV source which is evident $\sim 0.5^\circ$ north of Cyg X-3. An event-by-event centre of gravity (COG) calculation (Table 1a), weighting events with ± 1 from the s and αb regimes respectively is performed. The COG accuracy is limited by a systematic pointing error of $\sim 25''$ (Pühlhofer et al. 1997). A pre-trial significance at the COG position of $+5.9\sigma$ is obtained, summing events within $\theta = 0.12^\circ$ (Table 1b). Statistical trial factors arise from the initial discovery skymap (different to that in Fig. 1) in which event directions are independently summed in 1100 bins of size $0.1^\circ \times 0.1^\circ$. Assuming 1100 trials are accrued in locating the COG, the post-trial probability $P_t = 1 - (1 - P)^{1100}$ for P the pre-trial probability (one-sided $P = 1.9 \times 10^{-9}$, or $+5.9\sigma$), is then calculated as $P_t = 2.1 \times 10^{-6}$. This gives a post-trial significance of $+4.6\sigma$. 1100 is a slightly conservative trial estimate since oversampling of the γ -ray point spread function (PSF) by a factor ~ 1.5 occurs in the discovery skymap.

In order to verify results using the template model, we make use of a conventional type of background model employing background regions displaced spatially in the

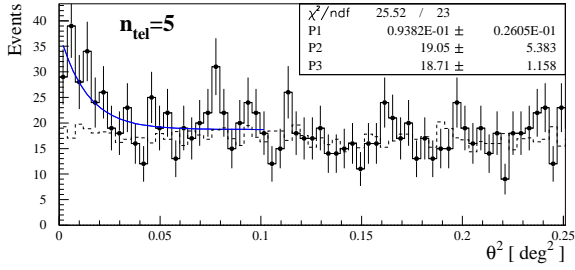


Fig. 2. Distribution of θ^2 for θ calculated from the COG (solid histogram & filled dots), against a background derived from the template model (dashed hist). The convolved radial Gaussian fit $F = P3 + P2 \exp(-\theta^2/(P1^2 + \sigma_{\text{pt}}^2))$ is indicated by the solid line with $P1 = \sigma_{\text{src}}$ the intrinsic source size. The PSF width $\sigma_{\text{pt}}=0.070^\circ$ is estimated from Crab data.

FOV from the on-source region but derived from the same $\bar{w} < 1.1$ regime. Here, background events are taken from ring-segments mirrored directly through each tracking position so as to match trigger characteristics of on-source data. A normalisation according to the solid angle ratio between background and on-source regions is then applied. This method accounts well for systematic differences in trigger characteristics or gradients across the FOV. Results are summarised in Table. 1b and are consistent with those from the template model.

2.2. Observational Properties of the TeV Source

Splitting data firstly according to their three tracking positions reveals commensurate source contributions (Table 1c). The source is also found to develop linearly with the cumulative number of background events. Such tests suggest consistency with a steady source during the three years of data collection. We have also verified that after cuts a constant background acceptance throughout the dataset is observed and that the event excess in \bar{w} -space appears consistent with that of a true γ -ray population. To determine source size, we fit a radial Gaussian convolved with the point spread function (determined from Crab data) to the excess events as a function of θ^2 , using a subset of events with the best angular resolution ($n_{\text{tel}} = 5$) for which minimal errors are expected (Fig. 2). The intrinsic size of the TeV source is estimated at $\sigma_{\text{src}} = 5.6' \pm 1.7'$ ($\sigma_{\text{src}} = P1 = 0.094^\circ \pm 0.026^\circ$). Due to correlations between the fit parameters the significance for a non-zero source size is at the $\sim 3.0\sigma$ level rather than the 3.5σ level indicated above. A breakdown of the excess with exclusive n_{tel} subsets also shows that the higher telescope-trigger multiplicities contribute greatest to the excess (Table 1d). Such behaviour is suggestive of a generally hard spectral index given that higher trigger multiplicities are favoured by higher energy events. For the energy spectrum calculation and selection cuts, we follow the method of Aharonian et al. (1999) using effective collection areas appropriate for on-axis and $\sim 1^\circ$ off-axis sources as per the expo-

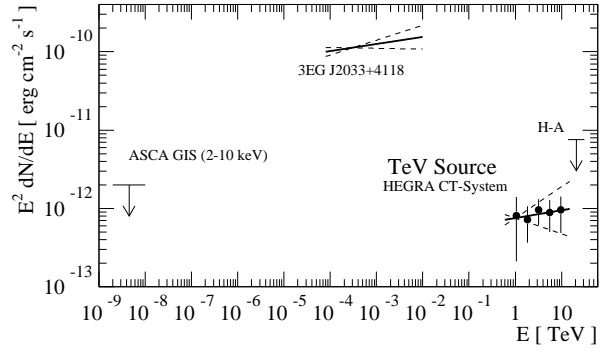


Fig. 3. Differential energy fluxes of the TeV source and other results. 'H-A' is the AIROBICC 90% confidence level upper limit (Prahla 1999) at the TeV COG converted to differential form at 20.8 TeV assuming a spectral photon index of -2.0 . We interpret the 3EG J2033+4118 flux here as an upper limit. The ASCA GIS 99% upper limit assumes a photon index of 2, and $N_H = 10^{22} \text{ cm}^{-2}$. Data fits (solid lines) and their 1σ statistical errors in photon index (dashed lines) are shown. TeV data are well fit ($\chi_\nu^2 = 0.23/3$) by a power law (Eq. 1)

sure efficiency for the TeV source in these data. A tight cut $\bar{w} < 1.1$, as opposed to the less-restrictive $\bar{w} < 1.2$ is also used. For energies below ~ 0.8 TeV the effective collecting area decreases markedly sharper at positions beyond $\sim 1.0^\circ$ off-axis compared to positions nearer on-axis. Limiting our fit therefore to energies > 0.8 TeV reduces systematic errors. A so-called loose cut $\theta < 0.224^\circ$ using the ring background model is used in deriving the energy bin-by-bin excess since a loose cut in θ improves the γ -ray selection efficiency according to the moderately-extended nature of the source. Results are shown in Table 1e and Fig. 3, with the spectrum being well fit by a pure power law with generally hard photon index. Systematic errors are estimated from changes in bin centres and uncertainties in Monte Carlo-derived collection areas:

$$\begin{aligned} dN/dE &= N (E/1 \text{ TeV})^\gamma \text{ photons cm}^{-2} \text{ s}^{-1} \text{ TeV}^{-1} \quad (1) \\ N &= 4.7 (\pm 2.1_{\text{stat}} \pm 1.3_{\text{sys}}) \times 10^{-13} \\ \gamma &= -1.9 (\pm 0.3_{\text{stat}} \pm 0.3_{\text{sys}}) \end{aligned}$$

3. Discussion & Conclusion

The OB association Cygnus OB2 is unique for its compact nature and extreme number of member OB and O stars (eg. Knödlseder 2000), and both theoretical and observational grounds for non-thermal particle acceleration have long-been discussed (eg. Montmerle 1979, Cassé & Paul 1980, Völk & Forman 1982, White & Chen 1992). The TeV source is positioned inside the core of Cygnus OB2 as defined by Knödlseder (2000). Assuming the TeV source is as distant as Cygnus OB2 (1.7 kpc), a luminosity $\sim 10^{32} \text{ erg s}^{-1}$ above 1 TeV is implied, well within the kinetic energy (KE) budget of Cygnus OB2 estimated

recently by Lozinskaya et al. (2002) at $\text{few} \times 10^{39} \text{ erg s}^{-1}$, and also within the KE budget of a number of notable member stars (eg. Benaglia 2001, Massey & Thompson 1991, Manchanda et al. 1996). So far no counterparts at other wavelengths are identified. No massive or luminous Cygnus OB2 star of note discussed recently (eg. Massey & Thompson 1991, Herrero et al. 2001, Benaglia et al. 2001) is positioned within the 1σ TeV error circle. No catalogued X-ray source from the ROSAT all-sky and pointed survey lies within the 2σ TeV error circle. Our analysis of archival ASCA GIS data yields a 99% upper limit (2–10 keV) of $2.0 \times 10^{-12} \text{ erg cm}^{-2} \text{ s}^{-1}$ (Fig. 3). Such results may imply that the energy source for particle acceleration is not co-located with the TeV source, arising instead from the winds of the young/massive stars of Cygnus OB2, either individually or collectively, or from an alternative source. The former scenario would generally favour accelerated hadrons interacting with a local, dense gas cloud, giving rise to π^0 -decay TeV emission. The likely hard TeV spectrum can be explained by (energy-dependent) diffusion effects, accelerator age, and accelerator to target distance (see eg. Aharonian 2001). There is however at present no strong indication from CO and HII surveys (Leung & Thaddeus 1992, Dame et al. 2001, Comeron & Torra 2001) for any localised dense gas cloud. A suggested alternative scenario involves a jet-driven termination shock at which accelerated electrons produce synchrotron and TeV inverse-Compton (IC) emission (Aharonian & Atoyan 1998). Such a jet could emanate from a nearby microquasar, possibly a class of high energy γ -ray sources (see eg. Paredes et al. 2000). In fact two nearby sources, 3EG J2033+4118 and also the EGRET source possibly associated with Cyg X-3 (Mori et al. 1997) could be GeV indicators of such a microquasar. We interpret the flux from 3EG J2033+4118 presently as an upper limit at the TeV COG (Fig. 3). Remarkably Cyg X-3 appears to have a bi-lobal jet (Marti et al. 2001) well-aligned with the TeV source, the latter which would be $\sim 70\text{pc}$ from Cyg X-3 in absolute terms if it is at the same distance ($>8.5 \text{ kpc}$). Note that future X-ray observations will be a crucial constraint on the IC emission in this context. Finally we should note that earlier claims for a TeV source (Neshpor et al. 1995, at a ~ 1 Crab flux level) and flaring episodes coincident with a Cyg X-3 radio flare at energies $>40 \text{ TeV}$ (Merck 1993, Krawczynski 1995) positionally consistent with our TeV COG have been reported. These results are however in conflict with our estimates of the flux level and steady nature of the TeV source assuming they all have the same origin. Further observations with the HEGRA CT-System aimed at confirmation and improving our spectral and source morphology studies are now underway.

Acknowledgements. The support of the German ministry for Research and technology BMBF and of the Spanish Research Council CICYT is gratefully acknowledged. We thank the Instituto de Astrofísica de Canarias for the use of the site and for supplying excellent working conditions at La Palma. We gratefully acknowledge the technical support staff of the

Heidelberg, Kiel, Munich, and Yerevan Institutes. GPR acknowledges receipt of a von Humboldt fellowship.

References

- Aharonian F.A., Akhperjanian A.G., Barrio J.A. et al. 1999 A&A 349, 11
 Aharonian F.A. 2001 Space. Sci. Rev. 99, 187
 Aharonian F.A., Atoyan A.M. 1998 New. Astron. Reviews 42, 579
 Becker-Szendy R., Bratton C.B., Casper D. et al. 1993 Phys. Rev. D 47, 4203
 Benaglia P., Romero G.E., Stevens I.R., Torres D.F. 2001 A&A 366, 605
 Cassé M., Paul J.A. 1980 ApJ 237, 236
 Comeron F., Torra J. 2001 A&A 375, 539
 Dame T.M., Hartmann D., Thaddeus P. 2001 ApJ 547, 792
 Daum A., Herman G., Hess M., et. al 1997 Astropart. Phys. 8, 1
 Herrero A., Puls J., Corral L.J. et. al 2001 A&A 366, 623
 Hofmann W., Jung I., Konopelko A. et.al 1999 Astropart. Phys. 10, 275
 Knödlseher J. 2000 A&A 360, 539
 Konopelko A. 1995, in Proc. Towards a Major Čerenkov Detector IV (Padova), 373
 Konopelko A., Hemberger M., Aharonian F.A., et al. 1999, Astropart. Phys. 10, 275
 Krawczynski H. 1995, Diploma Thesis, University of Hamburg
 Lamb D.Q., Macomb D.J. 1997, ApJ 488, 872
 Leung H.O., Thaddeus P. 1992 ApJS 81, 267
 Li T.P., Ma Y.Q. 1983 ApJ 272, 317
 Lozinskaya T.A., Pravdikova V.V., Finoguenov A.V. 2002 Astron. Letters 28, 223
 Manchanda R.K., Polcaro V.F., Norci L., et. al 1996 A&A 305, 457
 Marti J, Paredes J.M., Peracaula M. 2001 A&A 375, 476
 Massey P., Thompson A.B. 1991 AJ 101, 1408
 Merck M., 1993 Ph.D. Dissertation, Ludwig-Maximilians University Munich
 Montmerle T. 1979 ApJ 231, 95
 Mori M., Bertsch D.L., Dingus B.L. et al. 1997 ApJ 476, 842
 Neshpor Y.I., Kalekin O.R., Stepanian A.A. et. al 1995 Proc. 24th ICRC (Rome) 2, 1385
 Paredes J.M., Marti J., Ribo M., Massi M. 2000 Science 288, 2340
 Prah J. 1999 Ph.D. Dissertation, Universität Hamburg
 Pühlhofer G., Daum A., Hermann G. et. al 1997 Astropart. Phys. 8, 11
 Romero G.E., Banaglia P., Torres D.F. 1999 A&A 348, 868
 Rowell G.P. 2002 *in preparation*
 Völk H.J., Forman M. 1982 ApJ 253, 188
 White R.L., Chen W. 1992 ApJ 387, L81

(a) Centre of Gravity

RA α_{2000} :	20 ^{hr} 32 ^m 07 ^s	$\pm 9.3_{\text{stat}}^{\text{s}}$	$\pm 2.2_{\text{sys}}^{\text{s}}$
Dec δ_{2000} :	41° 30' 30''	$\pm 2.0'_{\text{stat}}$	$\pm 0.4'_{\text{sys}}$

(b) Tight cuts: $\theta < 0.12^\circ$, $\bar{w} < 1.1$, $n_{\text{tel}} \geq 3$

Background	s	b	α	$s - \alpha b$	S
Template	523	2327	0.167	134	+5.9
Ring	523	4452	0.089	128	+5.9

(c) Tight cuts on tracking subsets

Back.	t	η	s	b	α	S
— Cyg X-3 $\delta - 0.5^\circ$ —						
Template	39.5	0.69	148	647	0.172	+3.0
Ring			148	1994	0.057	+3.3
— Cyg X-3 $\delta + 0.5^\circ$ —						
Template	45.4	1.00	276	1214	0.170	+4.2
Ring			276	1266	0.168	+3.8
— GeV J2035 —						
Template	28.0	0.68	99	472	0.156	+2.6
Ring			99	1193	0.057	+3.4

t : Observation time (hrs)

η : Estimated γ -ray trigger effic. *cf.* on-axis.

(d) Tight cuts on n_{tel} subsets

Back.	s	b	α	$s - \alpha b$	S
— $n_{\text{tel}} = 2$ —					
Template	387	865	0.433	12	+0.8
Ring	387	4619	0.082	8	+0.5
— $n_{\text{tel}} = 3$ —					
Template	272	904	0.224	70	+4.1
Ring	272	2691	0.086	41	+2.6
— $n_{\text{tel}} = 4$ —					
Template	133	774	0.130	32	+2.9
Ring	133	1110	0.088	44	+3.2
— $n_{\text{tel}} = 5$ —					
Template	118	777	0.089	50	+5.1
Ring	118	651	0.102	52	+5.4

(e) Spectral Cuts[†]: $\theta < 0.224^\circ$, $\bar{w} < 1.1$, $n_{\text{tel}} \geq 3$

Back.	s	b	α	$s - \alpha b$	S
Ring	366	3222	0.087	86	+4.7

[†]: Aharonian et al. 1999 summarise other spectral analysis cuts.

Table 1. Summary of numerical results for the TeV source, comparing the two background models used for deriving excess significance. Here, s and b are the resulting event numbers for the γ -ray-like and background \bar{w} regimes respectively, and $s - \alpha b$ is the derived excess using a normalisation α . S denotes the excess significance using Eq. 17 of Li & Ma (1983). See section 2 for definitions of θ and \bar{w} .